

Thermoelectric Power Conversion using Generation of Electron-Hole Pairs in Large Area p-n Junctions

G. Span¹, M. Wagner², S. Holzer², T. Grasser²

¹ SAM – Span and Mayrhofer KEG, Bahnhofstr. 1, 6112 Wattens, Austria

² Institute for Microelectronics, TU-Wien, Gusshausstr. 27-29, 1040 Wien, Austria

Abstract

A new method for thermoelectric power generation using large area pn-junctions is presented [1]. Normally, thermal generation of electron-hole pairs is avoided because of the deteriorating effects of the minority carriers on the efficiency in classical thermocouples. A temperature gradient applied along the pn-junction causes a flux of carriers from hot to cold due to the Seebeck effect, which introduces a reverse bias and thus thermal generation in the hot part of the pn-structure. The generation of electron-hole pairs leads to a multitude of new properties that can be used to enhance the efficiency of the energy conversion. The generation rate of electron-hole pairs is a highly adjustable parameter, which makes it possible to tailor thermoelectric elements and modules to given boundary conditions. This is achieved by changing the amount and distribution of generation centers and the shape of the temperature gradient as well as the choice of the material system. Due to the generation of electrons and holes, no contact on the hot side of the thermoelectric element is necessary. Limitations of the hot side temperature caused by mechanical stress due to different thermal expansion of different materials or by the solder or joining material are therefore non-existing. To describe these structures, an effective figure of merit Z_{eff} is calculated using the device simulator Minimos-NT [2].

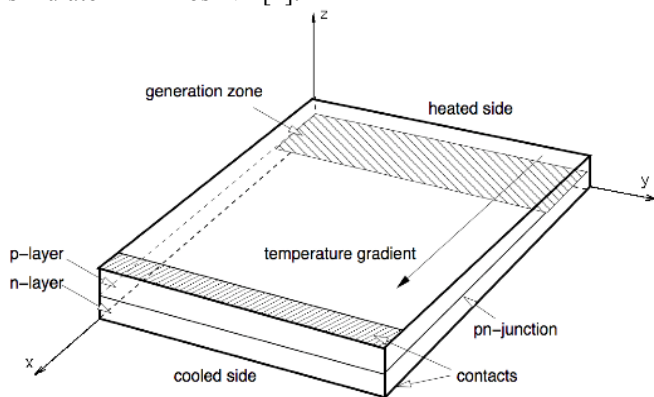


Figure 1: Large area pn-junction with applied temperature gradient. The thermal generation takes place on the hot side of the structure. Contacts are only present on the cold side.

Introduction

Increasing energy costs lead to a rising demand for alternative energy sources as well as new technologies for their efficient usage. A promising candidate for the near future is the direct conversion from heat to electricity using thermoelectric devices. This technology is already established in special space and remote environments, but the use of this technology on a broad basis requires more efficient and

reliable thermoelectric devices and modules. The future range of applications for these devices covers a great variety of thermal environments [1].

We present the physical background of our approach as well as simulation results for Si and SiGe structures, based on the comparison of experimental and simulated data for Si structures in [1]. The simulations are carried out using the device and circuit simulator Minimos-NT. A rigorous thermodynamical coupling of the heat system with the semiconductor equations is applied as proposed in [3]. The parameter modeling was ensured for the unusually large temperature range.

A sketch of our thermoelectric elements is shown in Figure 1, which basically consists of two layers, p- and n-doped with a large area pn-junction in between.

Thermal generation of electron-hole pairs takes place on the heated end of the structure (Fig. 1). The generated carriers are separated by the gradient of the built-in potential of the large scale pn-junction (Fig. 2). The built-in potential decreases with increasing temperature, which leads to a behavior of the electrostatic potential in the n- and p-layers similar to the Seebeck effect.

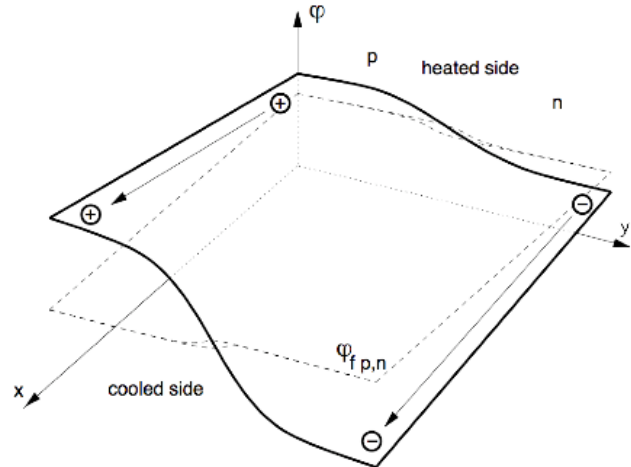


Figure 2: The electrostatic potential is affected by the local temperature. High temperatures decrease the potential difference across the pn-junction. The potential difference along the x axis causes a driving force to both carriers types from hot to cold.

A temperature gradient applied along the pn-junction causes a driving force to the free carriers from the hot to the cold part of the structure. The resulting current alters the local carrier balance between generation and recombination and leads to enhanced generation of electron-hole pairs in the hot part as well as increased recombination in the cold part of the structure. Contacts at the cooled end suppress this internal recombination in favor of an external current when connected to a load resistor. Hence, this device structure acts as a thermoelectric power source. This principle allows us to use

layered structures similar to solar cells as thermoelectric elements. In addition, it could be used to raise the efficiency of solar cells by using non uniform temperature distributions [4]. Thermoelectric modules can be manufactured by stacking these elements, similarly to [5].

Investigated Structures

The investigated structures consist of three layers, a heavily doped n-layer, an intrinsic layer, and a heavily doped p-layer. The generation takes places mainly in the intrinsic layer whereas the heavily doped layers act as transport channels. The structures have a width of 100 mm, are 20 mm long, and have an overall thickness of 2.4 mm. The considered doping profile is shown in Fig. 3.

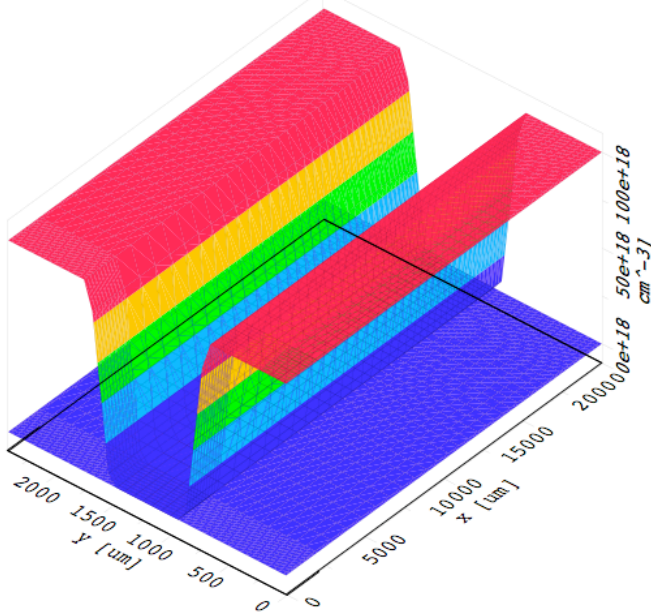


Figure 3: Dopant distribution in the investigated structures. The contacts are on the cold side (at $x=0$).

Thermal Generation

Thermal generation is described by the Shockley-Read-Hall formalism (Fig. 4). It is affected by the local temperature as well as the amount and energy level of present traps. For trap energy levels at the mid band gap, the thermal generation reaches its maximum. For Si, gold can be used as additional dopand in the generation region of the device to introduce deep levels close to mid band gap.

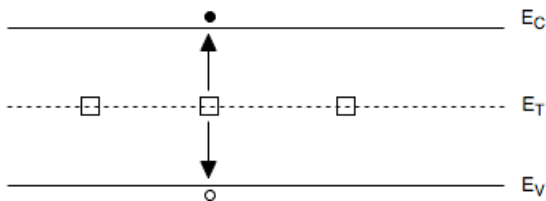


Figure 4: Trap assisted generation of electron hole pairs (Shockley-Read-Hall).

The impurity state can absorb differences in momentum between the carriers, therefore this generation process is the dominant one in Silicon and other indirect semiconductors.

The generation rate G can be calculated using [6]

$$G = \frac{n_i}{\tau_g},$$

$$\text{with } n_i = \sqrt{N_c N_v} \exp\left(-\frac{E_g}{2kT}\right),$$

$$\text{and } \tau_g = \frac{2 \cosh\left(\frac{E_t - E_i}{kT}\right)}{v_{th} \sigma_0 N_t}.$$

n_i ... intrinsic concentration, τ_g ... generation lifetime, N_c, N_v ... effective density of states in the conduction/valence band, E_g ... band gap energy, E_t ... energy of the traps, E_i ... intrinsic energy, v_{th} ... thermal velocity, σ_0 ... electron/hole capture cross sections, N_t ... trap density

The intrinsic density n_i of a material is a function of the band gap energy and depends exponentially on the temperature. This exponential dependence is the base for the presented thermoelectric generators. The strong non-linear behavior makes it possible to obtain net generation within a structure with a temperature gradient applied along the pn-junction. As a rule of thumb, thermoelectric generators based on thermal generation work at temperatures where the intrinsic density is of the order of 10^{16} cm^{-3} and above. Fig. 5 shows the intrinsic density for several semiconducting materials [6, 7].

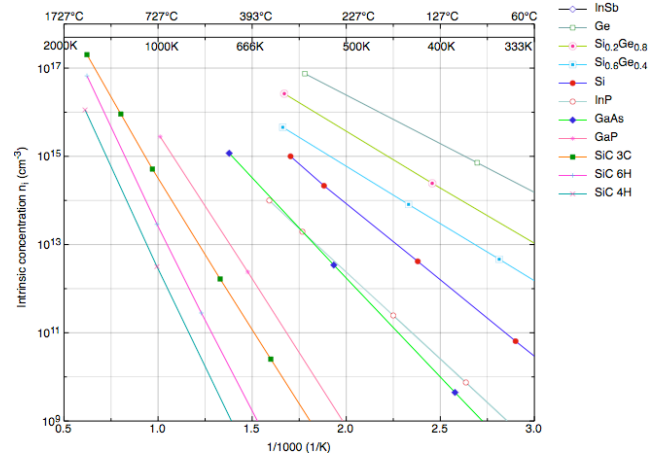


Figure 5: Intrinsic concentrations of several semiconducting materials as function of the temperature [6, 7].

To demonstrate the behavior of thermoelectric generators based on thermal generation at several modes of operation, three different scenarios are shown: the short circuit condition, generation at matched load, and open circuit condition. All scenarios were calculated by Minimos-NT and the output data were post-processed to create a visual representation. Electrons and holes are generated as pairs. The generation rate and electron current are shown in Fig. 6-11, the according hole current builds up symmetrically.

At short circuit condition, the thermal generation (Figure 6) and the electric current (Figure 9) become a maximum. The generation rate exceeds $10^{21} \text{ 1/s cm}^{-3}$, which translates to a current density of about 30 A/cm^2 . The recombination can be neglected.

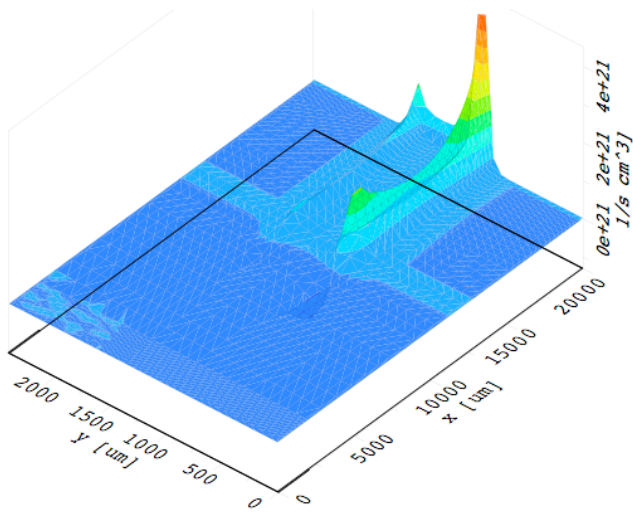


Figure 6: Electron generation rate at short circuit conditions. The rate reaches its maximum value, the recombination is at its minimum.

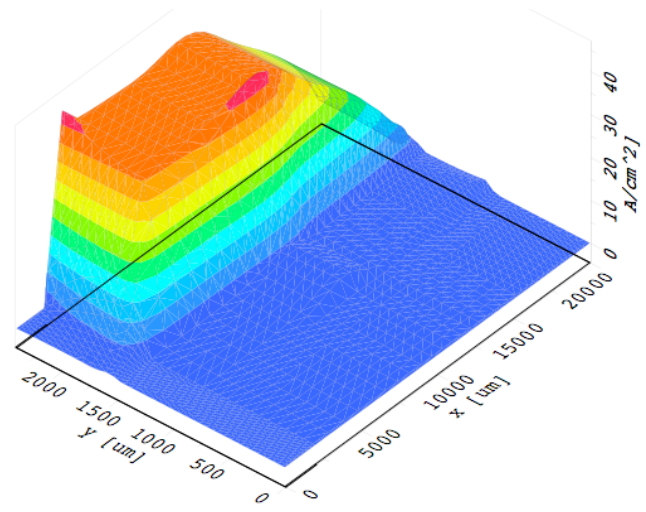


Figure 9: Generated electron current at short circuit conditions. The current accumulates in the generation zone and is almost constant along the transport region.

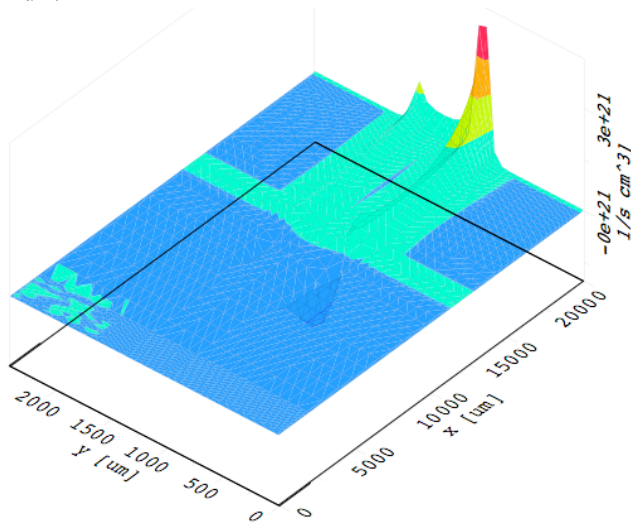


Figure 7: Electron generation rate at matched load. The generation is slightly decreased whereas the recombination is increased compared to the short circuit case.

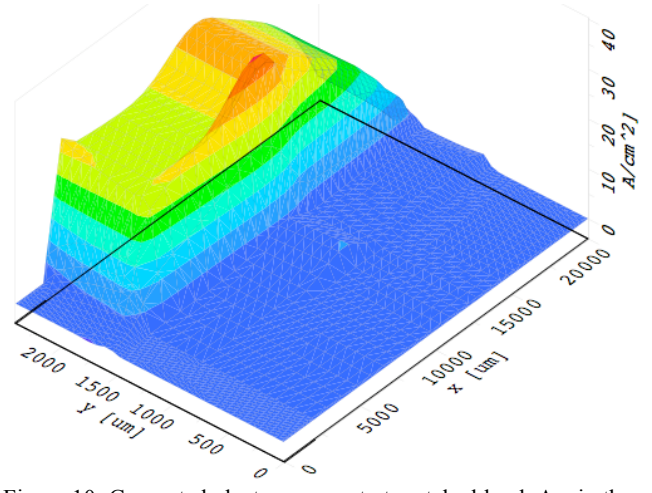


Figure 10: Generated electron current at matched load. Again the current accumulates along the generation zone, but the recombination decreases the current density along the transport zone.

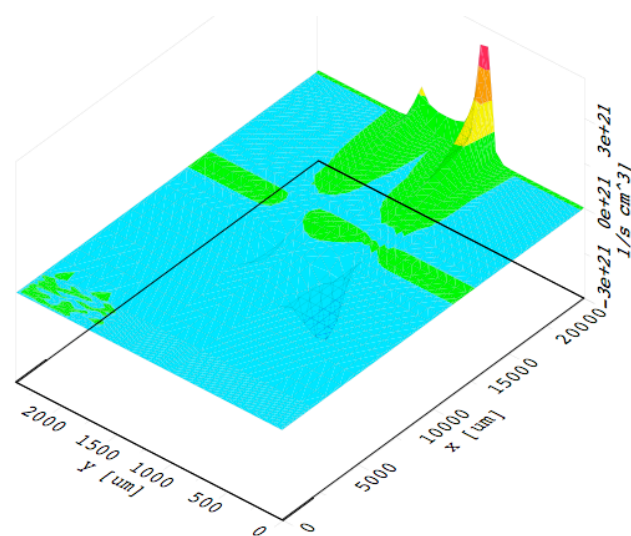


Figure 8: Electron generation rate at open circuit conditions. The total recombination is as large as the total generation.

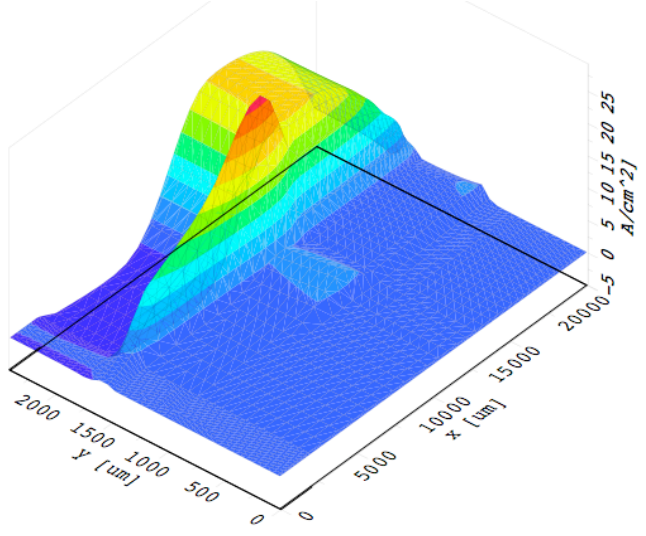


Figure 11: Generated electron current at open circuit condition. The current vanishes completely by recombination within the transport part of the structure. No current reaches the contacts.

At matched load condition the maximum power output can be expected. For the given structure the generation rate becomes smaller and the recombination increases (Figure 7 and Figure 10). The maximum current occurs within the structure and is the recombination current between the generated electrons and holes. This shows that the selected structure is not optimized and can be improved, which will be shown below.

At open circuit conditions all the generation and recombination takes place within the structure. In Figure 8 the generation rate is symmetrical and all the generated carriers recombines before reaching the contacts (Figure 11).

Influence of the temperature distribution

As seen before, the recombination of electron-hole pairs cannot be neglected and the generators have to be optimized for minimal recombination.

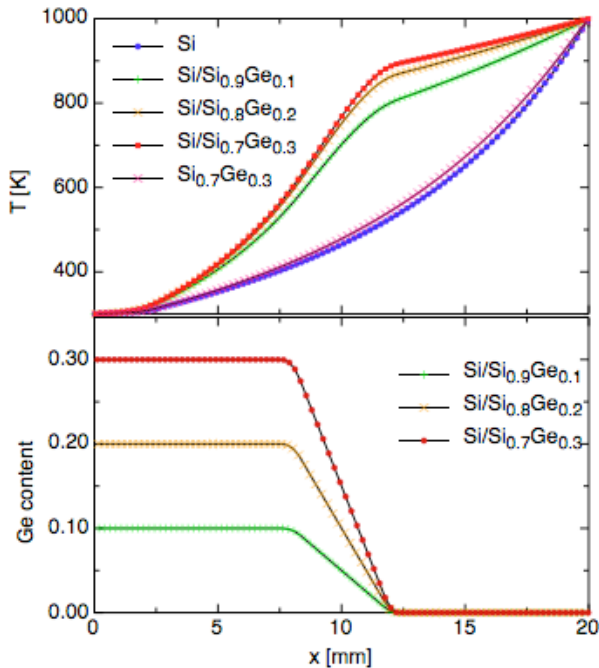


Figure 12: Ge distribution and resulting temperature gradient in sample 1 for three different SiGe compositions (10%, 20%, and 30%) at the cold side of the structure, the hot side consists of pure Si. The temperature distribution for pure Si and pure $\text{Si}_{0.7}\text{Ge}_{0.3}$ structures are shown as well.

One possibility to reduce the total recombination throughout the structure is to use the exponential dependence of the generation and recombination rate on the temperature. The recombination can be suppressed by having a steep temperature gradient so that only a small volume of the structure is warm enough for substantial recombination currents. On the other hand, in order to intensify the generation, it is of advantage to have a temperature gradient with a shallow slope at the hot side.

This desired bent temperature distribution can be achieved by geometrical engineering or the use of a combination of materials with different heat conductivities, such as Si and SiGe. Using Si with its high heat conductivity on the hot side

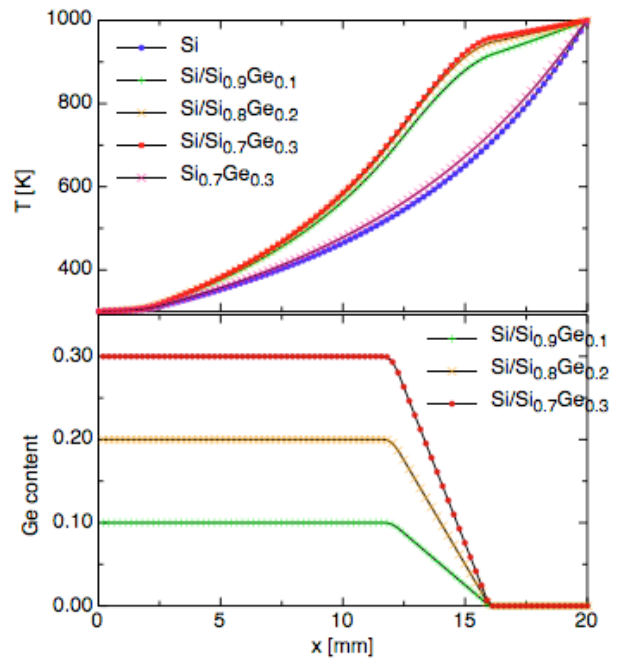


Figure 13: Ge distribution in sample 2 with resulting temperature gradients. Compared to sample 1, the pure Si part is shorter.

causes a low temperature drop while the low heat conductivity of SiGe provides the conditions for a steep temperature gradient in the cold part of the structure.

Four different configurations (Figures 12-15) of Si/SiGe structures with varying Ge content and distribution were simulated with Minimos-NT. They show that it is possible to generate more electric power while reducing the heat flux considerably compared to pure Si. Compared to pure SiGe structures it is possible to generate more electric current with almost the same thermal conductivity, resulting in a higher efficiency. Additionally, a variation of sample 4 was used to calculate the influence of additional deep trap levels that act as generation centers within the Si part of the structure on the hot side (sample 4+). In Figure 16 the combined results of the simulation runs are presented. For every sample, the influence of the Ge content was investigated. The pure Si structures show the lowest efficiency of about 0.4% because of the very high heat flux. The main contribution to higher efficiencies is the reduced thermal conductivity. As expected, the lowest thermal conductivity was found for the pure SiGe device, but not the highest power output and conversion efficiency. As described above, a bent temperature gradient increases the power generation considerably. For all samples the highest power output can be found for 10% Ge content, but the thermal conductivity is too high to achieve good efficiencies. For this structure the best efficiency can be found for 30% Ge content, depending also on the transport parameters which change with varying Ge content.

From sample 1 to sample 3, the pure Si part of the structure becomes shorter, so that the heat conductivity decreases. Because of the decreasing mobilities, the power output also decreases. The result is an almost constant efficiency for the three samples. In sample 4 (Fig. 15) the Ge content decreases with a shallower slope compared to sample 1 to 3.

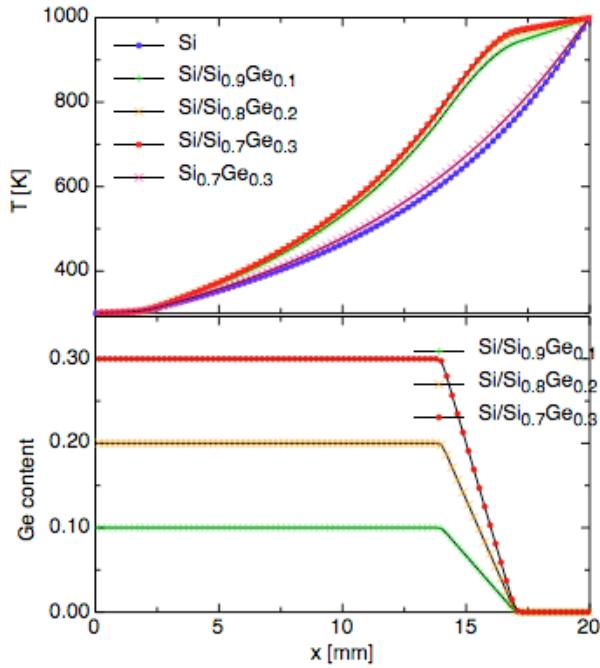


Figure 14: Sample 3 with the shortest Si part.

The resulting temperature gradient has a less pronounced bend and also the steep gradient is less bowed down. Because the local temperature determines the local electrostatic potential, such a temperature gradient leads to a more favorable potential gradient for the transport of carriers. This means that sample 4 has higher power output and efficiency than the three other samples.

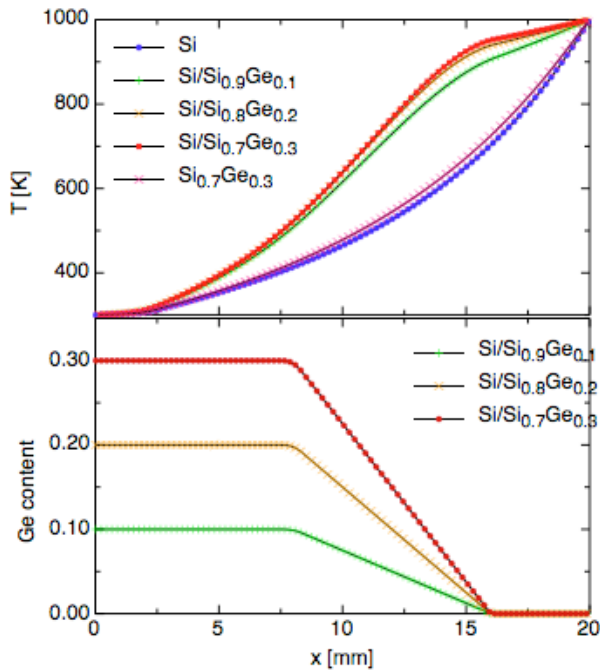


Figure 15: Sample 4 with short Si region, but smoother transition from zero to full Ge-content.

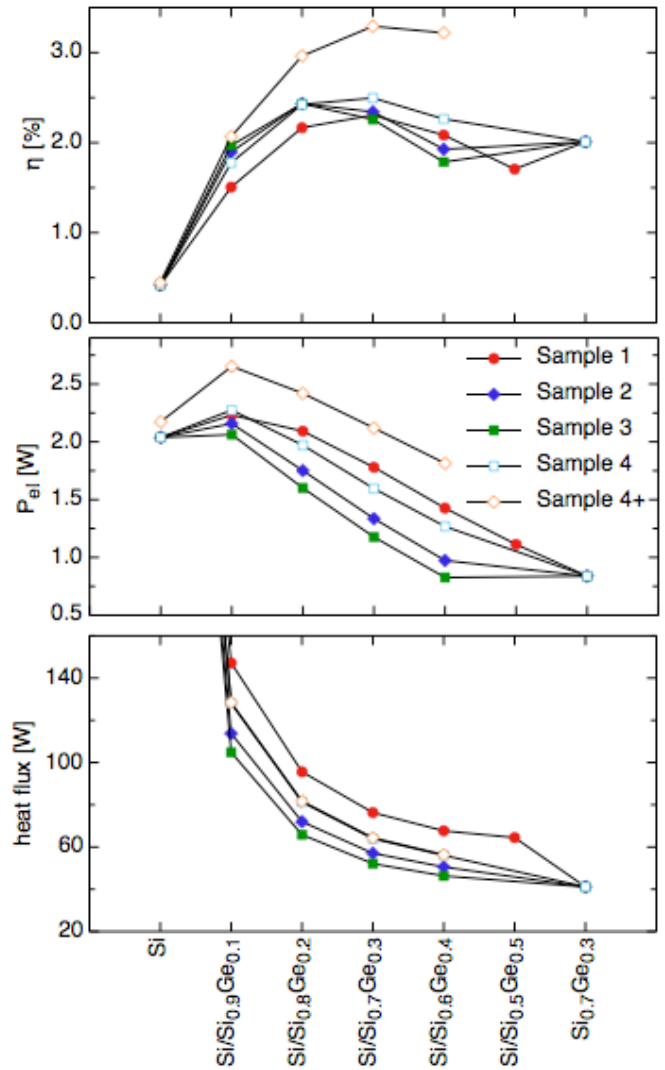


Figure 16: Power output, heat flux, and efficiency of the four structures with different Ge distribution. The device made from pure Si has a heat flux of 485W (value not shown in the figure).

To show the influence of deep trap levels acting as generation centers, additional dopands were added to sample 4, which became sample 4+. No other properties were changed. The result can be seen in Figure 16.

The power output at the highest efficiency increases from $P_{el} = 1.59$ W to $P_{el} = 2.12$ W, and since the thermal conductivity is practically unchanged, the efficiency increases from 2.5% to 3.3%.

Effective Z

To characterize the devices, an effective integral figure of merit Z_{eff} is calculated after [8] using

$$Z_{eff} = \frac{J_{sc} V_{oc}}{Q_0 \Delta T}$$

Q_0 is the zero-current heat flux, ΔT the temperature drop across the device, J_{sc} the short-circuit current, and V_{oc} the open-circuit voltage.

	Si	Si/ /Si _{0.8} Ge _{0.2}	Si/ Si _{0.7} Ge _{0.3}	Si/ Si _{0.6} Ge _{0.4}	Si _{0.7} Ge _{0.3}
Z _{eff}	2.39e-5	1.42e-4	1.47e-4	1.32e-4	1.18e-4
Z ⁺ _{eff}	2.56e-5	1.74e-4	1.93e-4	1.88e-4	

Table 1: Effective figure of merit Z_{eff} for Sample 4 and Z⁺_{eff} for Sample 4+ at several Ge contents.

Table 1 shows the calculated values of Z_{eff} for sample 4 and 4+. The highest Z_{eff} is found for the Si/Si_{0.7}Ge_{0.3} device and is about 20% higher than for the pure Si_{0.7}Ge_{0.3} device. Z⁺_{eff} is the effective figure of merit for sample 4+ with increased number of deep trap levels in the hot part of the device, which act as generation centers.

The value of Z_{eff} for the pure Si_{0.7}Ge_{0.3} device is lower than the published values of Z for Si_{0.7}Ge_{0.3} due to several reasons:

- Simulations are done for single crystal devices, which have a higher thermal conductivity than fine-grained (sintered) material.
- The geometry of the devices and transport layer thicknesses are not optimized yet.
- Recombination is still present.

By taking those reasons into account, Z_{eff} is in agreement with the published values for Z of SiGe [9].

Heat flux and power density engineering

In Figure 16, it can be seen that devices with different Si/SiGe partitioning have roughly the same conversion efficiency while the heat conductivity and power output vary about a factor of two. This behavior can be used to adjust the power and heat flux density to given boundary conditions while maintaining the same geometry of the generator or to reduce costs by changing the geometry but not the conversion efficiency.

The large amount of design parameters allows a good adjustment of large area pn-junction thermoelectric generators to specific thermal and geometrical environments. Due to the complex correlations within the device, we apply the state-of-the-art optimization framework SIESTA [10] in conjunction with Minimos-NT.

Siesta offers several interchangeable optimization algorithms as well as the possibility for designs of experiments.

Conclusions

It was shown that thermoelectric generators can be built using thermal generation of electron-hole pairs in pn-junctions instead of hot side contacts. Without those contacts, high temperatures can be exploited without the limiting factors of mechanical stress and fatigue.

The shape of the thermal gradient has a remarkable influence on the power output and efficiency of the presented generators. The enhancement of the electrical current suggests that an additional factor to drift currents is present. Since the carrier concentration varies between the transport part with a steep thermal gradient and the generation part of the structure

with roughly constant temperature, occurring diffusion currents play a significant role.

The enhancement of the power output and power density is contrary to most current research efforts, which focus on the lowering of the thermal conductivity. By combining both ideas, the efficiency of thermoelectric generators can be increased remarkably.

The versatile properties of our generator concept allow adjusting thermoelectric generators to almost any boundary conditions by help of the optimization framework SIESTA in combination with the device simulator Minimos-NT.

Acknowledgments

We acknowledge financial support through the FFG, the Austrian Research Promotion Agency (Österreichische Forschungsförderungsgesellschaft) for project no. 809975 (SAM) and project no. 810128 and the local government (Impulspaket Tirol).

References

1. G.Span, M.Wagner, T.Grasser, *Proceedings ECT2005*, p. 152
2. IµE, MINIMOS-NT 2.1 User's Guide, Institut für Mikroelektronik, Technische Universität Wien, Austria, (2004).
3. G. Wachutka, *IEEE Trans. CAD*, 9, 1141 (1990).
4. S. Kettemann, and J.-F. Guillemoles, 16th Workshop on Quantum Solar Energy Conversion, Bad Gastein, Austria, (2004).
5. C.S. Tan, A. Fan, K.-N. Chen, and R. Reif, 7th Annual Topical Research Conference on Reliability, Austin, Texas, (2004).
6. Sze, S. M., Semiconductor Devices, Physics and Technology, John Wiley & Sons, 1985
7. Ioffe Physico-Technical Institute, Electronic Archive "New Semiconductor Materials, Characteristics and Properties", <http://www.ioffe.rssi.ru/SVA/>
8. P.L.Hagelstein, Y.Kucerov, *Applied Physics Letters*, 81(3), 2002, p. 559.
9. Rowe, D. M., CRC Handbook of Thermoelectrics, CRC Press Inc., 1995
10. SIESTA 1.1std, Institut für Mikroelektronik, Technische Universität Wien, Austria, (2003).